

Structurally Constrained Anisotropic Multi-Wave-Inversion Utilizing Machine Learning and Big Data on a Middle East OBC Project

V. Prieux¹, T. Bardainne¹, A. Meffre¹, H. Prigent¹, F.J. Van Kleef², M. Waqas², L. Hou²

¹ CGG; ² ADNOC Offshore

Summary

Challenged by the presence of strong anisotropy and velocity reversals in the near surface, we apply structurally constrained anisotropic multi-wave inversion (MWI), over 1200 km² of OBC data offshore Abu Dhabi. MWI aims to simultaneously invert the P-wave first breaks (FB), the ground roll dispersion curves (DC) and the vertical two-way times (VTWT) of the main interfaces. In this study, MWI is extended to invert for the Thomsen's anisotropic parameter ϵ that is constrained by the FB and the VTWT. The high resolution V_p and ϵ obtained from MWI greatly contribute to the velocity model building. Additionally, geomechanical parameters like the uniaxial compressive strength (UCS) are also derived from the combination of V_p and V_s .

We highlight the importance of proper preconditioning of the DC and FB inputs using data mining tools when applying the method to a large production dataset. Machine learning (ML) is used to better account for the vertical and horizontal geological variability of the survey in picking the phase velocity, while data mining tools allow interactive QC and editing of the FB picks on large data sets.

Introduction

The complexity of the Middle East near-surface has led the oil and gas industry to seek advanced and innovative solutions to overcome this challenge. Properly imaging the near surface is very important in velocity model building as shallow velocity errors propagate into deeper layers. The case study described here concerns a major oilfield offshore Abu Dhabi. A 3D 4C OBC seismic dataset was acquired in 2014 in a very shallow water environment. The near surface is characterized by sharp velocity reversals and strong anisotropy.

Conventional methods have consistently failed to properly image the very near subsurface. First break (FB) tomography is not able to resolve the subsurface with multiple shallow reversals, as it cannot discriminate between depth and velocity to satisfy arrival times. Reflection tomography is not applicable either because of the lack of offsets in the very shallow and the weak signal-to-noise ratio (SNR). In this study, we use the structurally constrained multi-wave inversion (MWI) approach proposed by Bardainne (2018) to solve the complexity of the very near subsurface. MWI is a simultaneous inversion of P-wave FB, ground roll dispersion curves (DC), and Vertical Two-Way Times (VTWT) of the main interfaces. These complementary and redundant sources of information feed a multi-parameter joint inversion algorithm, which is better determined than a sequential inversion of the same inputs. MWI provides high resolution layered velocity models, structurally consistent with the reflectivity. It also has the potential to detect velocity reversals when slope breaks are picked on the fundamental mode of the DC (white arrow in Figure 1b). Maslet et al., (2018) have shown that efficient machine learning (ML) driven analysis of the DC is crucial to stabilize the inversion. In this study, we further extend the use of big data tools to the selection of FB picks. Another novelty is that the Thomsen's anisotropic parameter ε is also inverted by MWI, mainly constrained by the combination of FB with VTWT.

Besides the recovery of V_p , V_s and ε parameters and improved imaging, we also illustrate an added value of MWI through the estimation of geomechanical uniaxial compressive strength (also called unconfined compressive stress, or UCS).

Method

The VTWT are picked along two main Tertiary reflectors on a pre-stack time migration (PSTM) stack, namely Lower Fars and Dammam horizons (in black in Figure 4). The VTWT are key to constrain the structure and to recover ε , hence the method's name 'structurally constrained anisotropic MWI'. ε is known to be determined by the ratio of the horizontal P velocity, coming from the FB, over the vertical P velocity. In MWI, the average vertical velocity at an interface is equal to its depth over the VTWT. The MWI process jointly adjusts the velocity and the depth of the horizons to satisfy the VTWT and therefore constrains the structure. This new ability of MWI to invert for ε allows for consistency between the VTWT and the FB arrival times in the presence of anisotropy.

The ground roll DC were picked on the geophone component which showed better SNR at low frequencies than the hydrophone component. The data were sorted by cross-spread, and densified to a 6.25 x 6.25m bin size to ease the picking at higher frequencies. Only the fundamental mode of the DC was picked, the higher order harmonic modes are not yet being modelled in the scheme. To constrain the picking to a unique mode, velocity corridors representative of geological areas were designed based on unsupervised K-mean classification of the DC as recommended by Maslet et al., (2018).

Practical aspects

a) DC clustering per frequency:

The low frequencies of the surface waves propagate deeper than the high frequencies. The different frequencies are hence representative of different geological layers. By clustering on different frequency ranges, we improve detection of geological changes with depth as displayed by Figure 1c-e. Moreover, it guides the picking to focus on the strong curvature of the DC at the very low frequencies. The latter are very important for MWI because they cover the whole penetration depth. To find the optimum number of classes for each frequency range, we start calculating self-organizing maps (SOM) on DC. SOM is a dimensionality reduction method preserving topological properties of the input space through competitive learning. Figure 1a displays the 2D-SOM for the low frequency

range, showing the 4 main classes in Figure 1c. The connectivity between the 256 classes can be visualized with the colored honeycomb in Figure 1a. The classes in white are intermediate ones and form the borders of the chosen classes. The colors are fairly homogeneous inside each class, indicating we have chosen the correct number of classes.

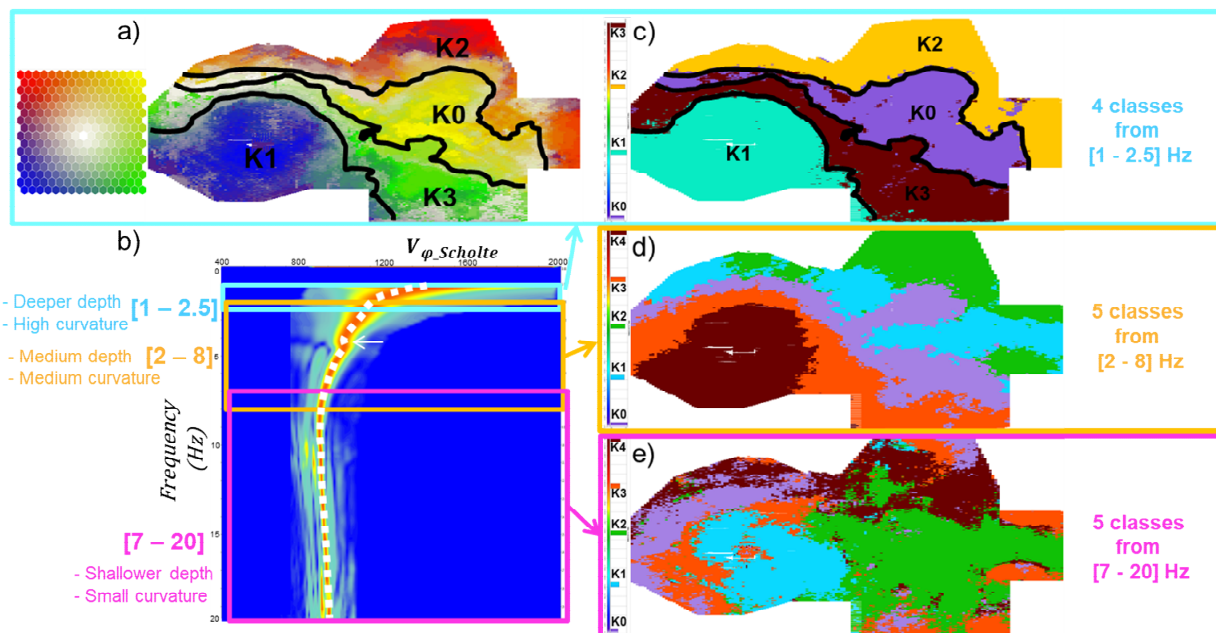


Figure 1: (a) is the result of a SOM from the lowest frequency range. (b) is an example of a DC where the picked velocity is delineated by the white dashed line. (c-e) are clustering maps over the survey using different frequency ranges of the DC (from low to high frequencies).

We illustrate in Figure 2 that the use of the clustering per frequency to guide the velocity corridors prevent us from picking the velocity reversals highlighted by the red ellipses. Although not shown here, we also observed that this ML strategy stabilizes the picking at the low and high frequency ends.

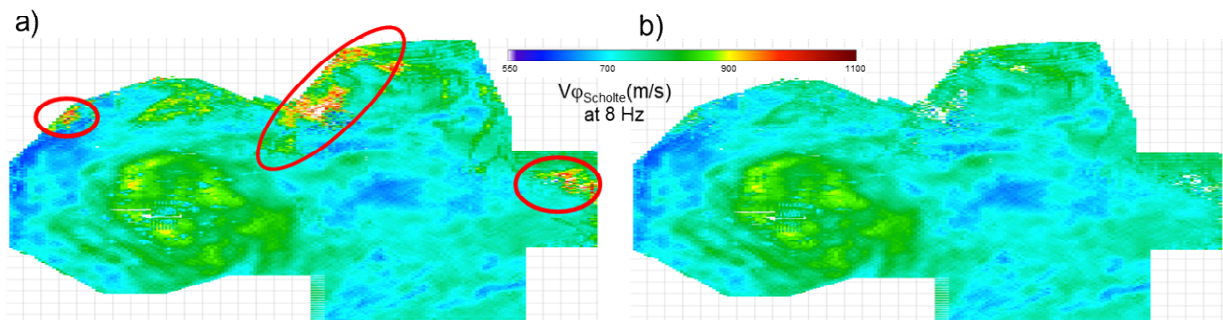


Figure 2: Scholte phase velocity map of the whole survey picked at the frequency of 8 Hz derived (a) without the help of ML and (b) when designing velocity corridors guided by a clustering by frequency. Note the anomalous velocity reversals in the red ellipses in (a).

b) FB editing:

The so-called “Christmas tree effect”, synonymous with a decrease in FB velocity with offset, is a well-known difficulty when picking the FB. This behavior occurs when there are alternating high and low velocity layers as described by Sun and Zhang, (2013). The MWI algorithm computes the P-wave travel-times of the refracted first arrivals using a finite difference Eikonal solver. The modelled first arrivals are often inconsistent with the picked FB because the amplitude of the FB is too weak to be picked, and the downward phase is picked instead. This inconsistency introduces a velocity bias in the tomographic result, as illustrated by Sun and Zhang (2013), which is also expected for MWI. To avoid the velocity bias related to the Christmas tree effect in our solution, we decided to remove the picks that showed a negative velocity derivative with offset. Our big data infrastructure allows for the efficient control of seismic attributes in all domains, and proved very useful to QC and edit the FB

picks for large datasets. We designed a velocity corridor in the velocity/offset domain (Figure 3a-b) to discard the picks representative of a velocity reversal, especially present at near and far offsets. Figure 3c and 3d show how bias was corrected and sharp high velocity anomalies were removed with this FB editing. Figure 3e and 3f display an example of FB velocity distribution inside receiver gathers before and after editing the picks.

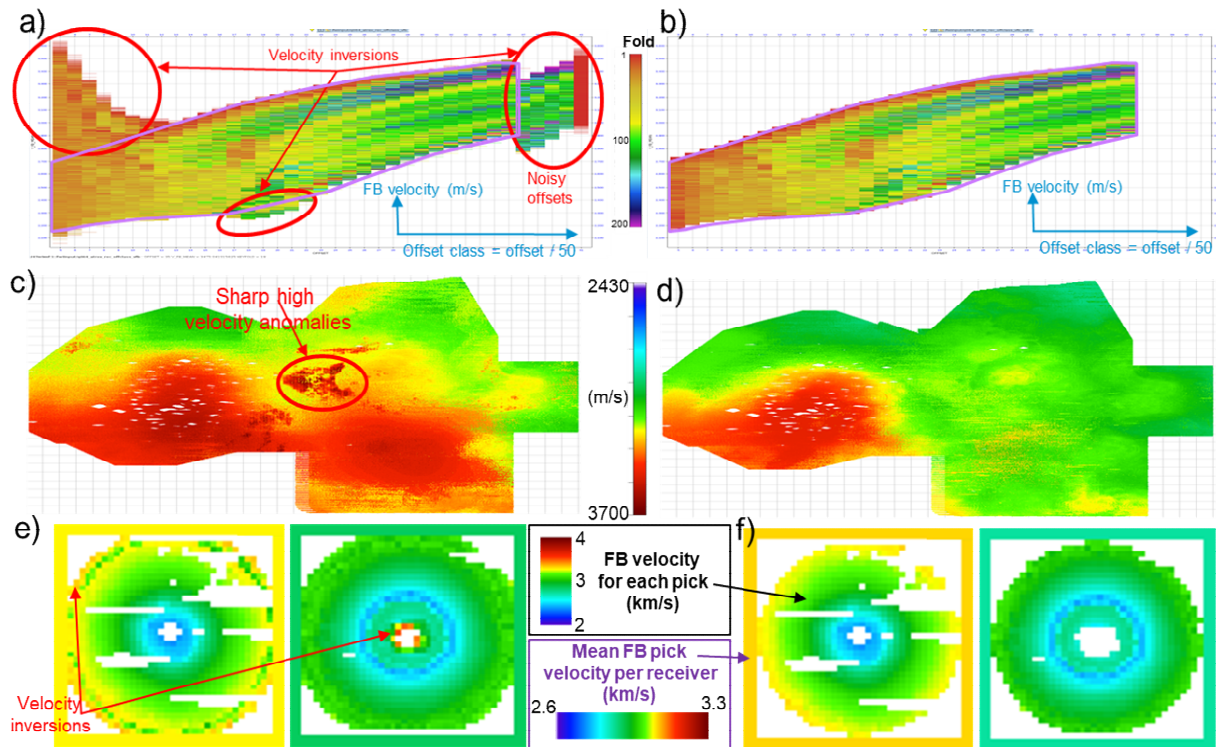


Figure 3: Visual QCs of the FB picks before editing in the left column, and after polygon selection (in purple in a,b) in the right column. (a,b) FB pick velocity is displayed with respect to the offset class. (c,d) Shot map of the maximum FB velocity per shot. (e,f) FB pick velocity distribution inside two receiver gathers.

MWI results

Figure 4 shows the inverted MWI models and their comparison with a sonic log. The MWI models conform to the general structure given by the two VTWT horizons (in black). MWI confirms the presence of high anisotropy as ϵ reaches a maximum of 27% (Figure 4g). The P and S velocity profiles follow the sonic trends accurately. MWI recovered the three velocity reversals (white arrows on velocity profiles), and a V_p/V_s reversal (red arrow).

The PSDM stacks in the starting models and the MWI models are shown in Figure 5. We observe an uplift in continuity and focusing of the reflectors inside the green ellipses.

The UCS parameter is often used in civil engineering as it is a measure of the layer stiffness. This can be of interest to evaluate the drilling risks. Here the UCS was derived from the MWI V_p and V_s parameters (Figure 6a) with the formula: $UCS \text{ (Mpa)} = 0.055 E^{0.6275}$, where E is the Young Modulus. By applying the geotechnical classification based on the range of the UCS values (Figure 6b), the presence of a weak layer can be detected (red arrow). This is also the layer that shows a reversal of the V_p/V_s ratio. Another stiffness reversal was observed between the black horizons (white arrow).

Conclusion

MWI is a multi-parameter inversion method which offers a solution for near-surface velocity model building in the presence of shallow velocity reversals and significant anisotropy. Machine learning and big data tools allow efficient QC and editing of the different inputs, crucial to stabilize the inversion. Our MWI application over a complete 1200 km² area allowed us to improve the overall imaging of the very near surface, to provide anisotropy estimation, a good match to the wells and rock property information.

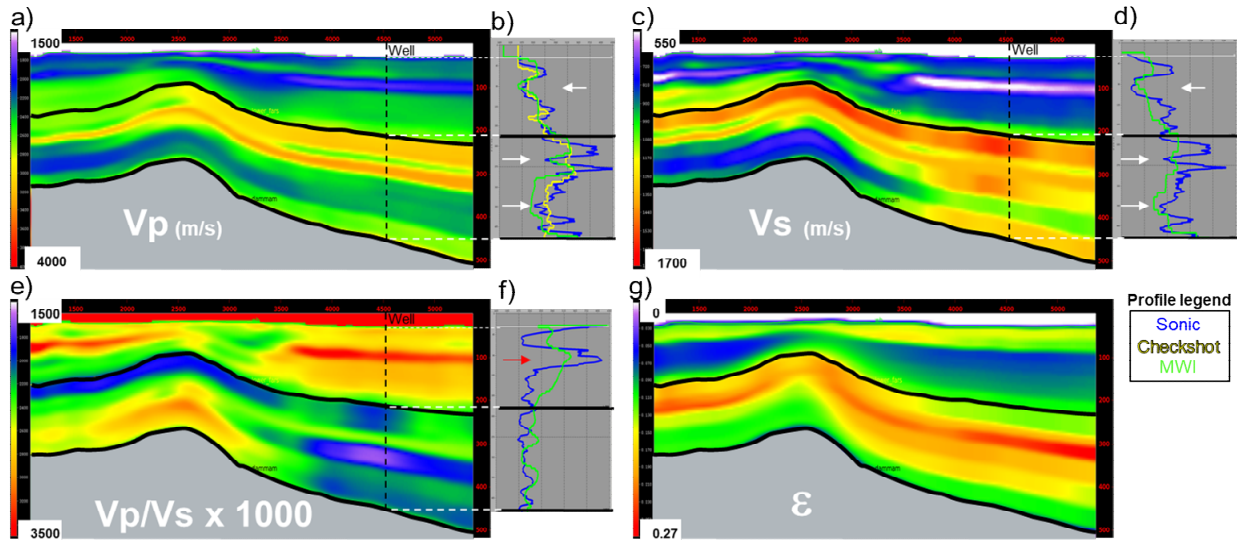


Figure 4: Inverted MWI models (a,c,e,g) and comparison with their respective log (b,d,f). The black dashed line indicates the crossline location of the well. The inline location of the well is offset from this section. The grey area is not inverted by MWI. Note on the velocity profiles the detailed velocity reversals found by MWI (white arrows).

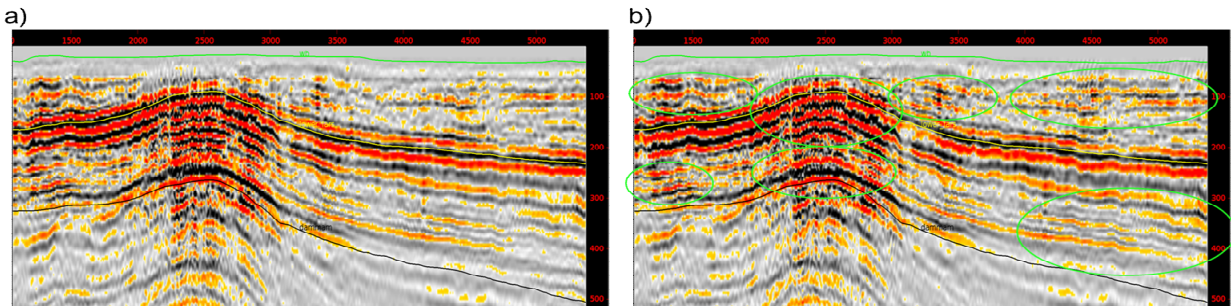


Figure 5: PSDM stack using the starting model (a) and the MWI model (b).

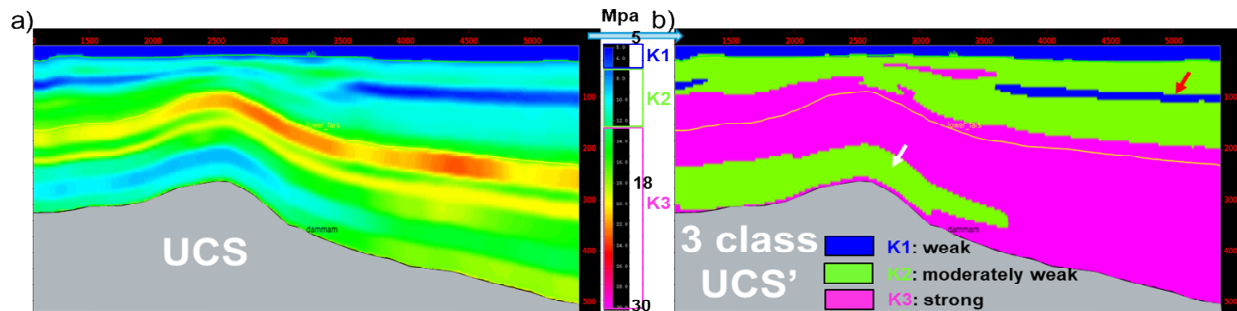


Figure 6: (a) UCS parameter derived from the V_p and V_s MWI parameters. (b) 3 class UCS model inferred from the range of UCS values, to clearly show the weak and the strong layers.

Acknowledgments

We would like to thank ADNOC Offshore for permission to publish these results.

References

- Bardainne, T. [2018] Joint inversion of refracted P-waves, Surface Waves and Reflectivity. 80th EAGE Conference & Exhibition
- Maslet, S., Bardainne, T., Massart, V. and Prigent, H. [2019] Near surface characterization in Southern Oman: Multi-Wave Inversion guided by Machine Learning. 81th EAGE Conference & Exhibition
- Sun, M. and Zhang, J. [2013] Understanding of the first arrivals in the shape of a Christmas tree. SEG International Exposition and Annual Meeting, Extended Abstracts.